Journal of Applied Physics

Cadmium telluride as a potential conversion surface

Cite as: J. Appl. Phys. **129**, 045303 (2021); https://doi.org/10.1063/5.0033701
Submitted: 18 October 2020 . Accepted: 12 January 2021 . Published Online: 29 January 2021

Jonathan Gasser, Martina Föhn, André Galli, Elisa Artegiani, Alessandro Romeo, and Peter Wurz

AIP Publishing

Journal of Applied Physics ARTICLE scitation.org/journal/jap

Cadmium telluride as a potential conversion surface

Cite as: J. Appl. Phys. **129**, 045303 (2021); doi: 10.1063/5.0033701
Submitted: 18 October 2020 · Accepted: 12 January 2021 ·
Published Online: 29 January 2021

Jonathan Gasser,[1,a)] Martina Föhn,[1] André Galli,[1] Elisa Artegiani,[2] Alessandro Romeo,[2] and Peter Wurz[1]

AFFILIATIONS

[1]Physics Institute, Space Research and Planetary Sciences, University of Bern, Sidlerstrasse 5, 3012 Bern, Switzerland
[2]Department of Computer Science, Laboratory for Photovoltaics and Solid State Physics, University of Verona, Strada le Grazie 15, 37134 Verona, Italy

[a)]**Author to whom correspondence should be addressed:** jonathan.gasser@space.unibe.ch

ABSTRACT

In instruments for low energetic neutral atom imaging of space plasmas, a charge state conversion surface (CS) is used to convert neutral atoms into ions for detection. We investigated a cadmium telluride (CdTe) coated sample as a novel material candidate regarding its suitability to be used as a CS. We measured the efficiency of converting H and O atoms into negative ions by surface scattering, as well as their angular scattering distribution, for energies from 195 eV to 1 keV at 8° incidence angle. Also, the energy distribution of scattered particles was recorded for incident O_2^+ ions, which confirms that molecules are mainly scattered as single atoms. The mean energy loss per atom was about 45%. The negative ion yield from scattering off CdTe was up to 13% for O and about 2% for H, which is comparable to other CS coatings in use. CdTe shows a nearly circular angular scattering cone of width comparable to established CS materials. We conclude that CdTe is a viable CS coating material for ENA instruments in space applications.

I. INTRODUCTION

Spaceborne instruments for energetic neutral atoms (ENAs) continue to be a highly relevant tool for interplanetary and interstellar space plasma research. Reviews on scientific techniques and instrumentation for imaging of space plasmas can be found in Gruntman,[13] Williams *et al.*,[38] and Wurz.[40] Several past and present space missions have been equipped with an ENA instrument at low energies, such as IMAGE,[22] Mars and Venus Express,[3,4] Chandrayaan-1,[2,6,16] and BepiColombo.[24] The well-known IBEX mission[9,20] has brought light on, among others, the global heliospheric structure by observing the plasma of the heliospheric interface via ENAs from Earth's orbit. While IBEX is expected to run until at least 2025, its successor mission the Interstellar Mapping and Acceleration Probe (IMAP) is currently under development,[21] with a low-energetic ENA camera being among the scientific instruments. Most recently, the upcoming JUICE mission (Jupiter Icy Moons Explorer)[10] by ESA also includes two ENA instruments for low- and high-energy ENAs in its particle environment package.[5]

All the low-energetic neutrals instruments for space research rely on an efficient method of ionization for the ENAs to electrically analyze the ENAs.[40] To date, in the low-energy range, the most widely used method and so far the only space-proven is via surface conversion: Neutral particles strike a highly polished charge-state conversion surface (CS) at a grazing angle of incidence and thereby pick up an electron while being scattered. An overview of negative ion sources and their application to accelerator physics and plasma research is given in Faircloth and Lawrie.[7]

The underlying physical theory of particle charge conversion upon surface scattering at a grazing incidence angle is still not understood in full detail. Quite a few theoretical models exist for special types of surfaces such as metals or alkali halides.[19,39] Negative ionization happens via resonant electron transfer from the crystal lattice to the incident atom's electron affinity level. Thus, a low work function in the surface material enhances electron transfer to the atom. However, diamond and other insulator surfaces with high work function showed comparably high negative ionization efficiency,[42] which are probably promoted by surface states.

The efficiency of converting neutral atoms into ions and the scattering properties strongly depend on the CS material. A high yield of negative ions and a narrow angular scattering cone both directly alter the instrument efficiency by improving the throughput of downstream ion-optical elements within the instrument. In space ENA imaging instruments, the CS should at least yield about 1% negative ions for the ENA species of interest (predominantly H and O). Even though this seems a low value, the 1% ion yield is required for an acceptable signal to background level, which is a key criterion especially in low-energy ENA instrumentation.[40] Compared, e.g., to electron impact ionization, with efficiencies of about 10^{-4}, this is still respectable for a passive ionization method. Moreover, this ionization method does not require electrical power, which is a big advantage for space instrumentation. In addition, CS materials for space applications should be chemically stable and mechanically robust on long time scales, without possibly hazardous components, show no degeneration or surface charging effects, and should be readily available at affordable cost. Various materials have been considered and investigated over the past decades (cf., Wurz *et al.*[41] and references therein).

Among the highest negative ion yields have been reported for aluminum oxide[26] (Al_2O_3) and diamond-like carbon[1,23,30,36] (DLC), conversion surfaces, which both have been successfully applied in several space missions, e.g., in BepiColombo[24] and IBEX.[9] Nevertheless, there is interest in finding potential CS materials offering improved conversion efficiencies, less angular scattering, and less energy scattering to achieve even better performance in future space instrumentation.

Cadmium telluride (CdTe) was chosen as a candidate surface material based on the high atomic mass of its two components, Cd and Te, compared to the atoms of interest in space plasma research. In the binary collision model, ion-surface scattering happens via a single ideal collision of the incident atom (mass m_1, kinetic energy E_i) with a surface atom (mass m_2) in the crystalline lattice at rest. The incident atom is scattered by the angle θ from its initial trajectory, thereby some portion (p_2', E_2') of the energy-momentum is transferred to the lattice atom. The relative amount of the incident atom's kinetic energy lost in the collision, $\delta E_i/E_i$, would then depend on the mass ratio according to

$$\frac{\delta E_i}{E_i} = \frac{E_2'}{E_i} = \frac{m_1}{m_2}\sin^2(\theta)\left(1+\frac{1}{4}\left(1-\frac{m_1}{m_2}\right)^2\sin^2(\theta)\right)+\mathcal{O}(\theta^6) \quad (1)$$

for small deflection angles θ. If applicable, this suggests that the energy transfer from the incident atom to the surface should be reduced for mass ratios m_2/m_1 much larger than one, as opposed to carbon or oxygen atoms in CS coating materials such as DLC or Al_2O_3 ($m_C/m_O \simeq 0.75$, $m_O/m_{Ne} \simeq 0.8$). For CdTe, the most abundant isotopes are ^{110}Cd, ^{111}Cd, ^{112}Cd, ^{114}Cd, ^{126}Te, ^{128}Te, and ^{130}Te, which yields mass ratios of $m_{Cd}/m_O \geq 6.8$ and $m_{Te}/m_O \geq 7.8$.

Moreover, CdTe is a II–IV semiconductor material. It has a crystalline sphalerite structure ($F\bar{4}3m$), a lattice constant of 6.48 Å, and a direct band gap of 1.56 eV. Its work function is about $\Phi = 5.7$ eV and the melting point is above 1300 K, and it is nearly insoluble in water. CdTe is widely used as an absorber material in thin film solar cells.[11,12] Alloyed with Hg or Zn, it makes an efficient infrared (IR), x-ray, or gamma ray detector material.[18,27,33,34] Furthermore, CdTe is used for IR optical windows and lenses. It, therefore, fulfils the aforementioned criteria to be considered a suitable CS material for space applications. Other similar semiconductor materials with the same crystal structure have a larger bandgap and reveal other disadvantages (e.g., ZnTe is flammable, CdSe is toxic and a suspected carcinogen, GaAs oxidizes over time, and ZnSe may react with acids to form toxic H_2Se). Despite its heavy metal component, the possible harmfulness of CdTe is very moderate and is further evaluated due to its wide application in photovoltaic research and production.

II. SETUP AND METHODS

A. ILENA test facility

The measurements were done in the Imager for Low Energetic Neutral Atoms (ILENA) test facility[35] at University of Bern. The ILENA setup consists of an electron impact ion source, a 90° sector magnet for ion species selection, a beam guiding system, a rotatable sample holder, and a movable two-dimensional imaging multichannel plate (MCP) detector with an angular field-of-view of 21° × 21° as seen from the sample center. A schematic overview of ILENA is shown in Fig. 1. The experimental setup is contained in a vacuum chamber equipped with a turbo molecular pump and an ion getter pump, which establish a base pressure in the low to mid-10^{-8} mbar range.

In the ion source, positive test gas ions are produced and extracted by a post-acceleration voltage of 100 V–3 kV. The ion beam is then focused and guided into the sector magnet, where the ion species of interest is selected by applying the appropriate magnetic field normal to the ion beam. The ion beam passes through a 1 mm diameter pinhole before it strikes the CS sample under an adjustable grazing incidence angle. In the scattering

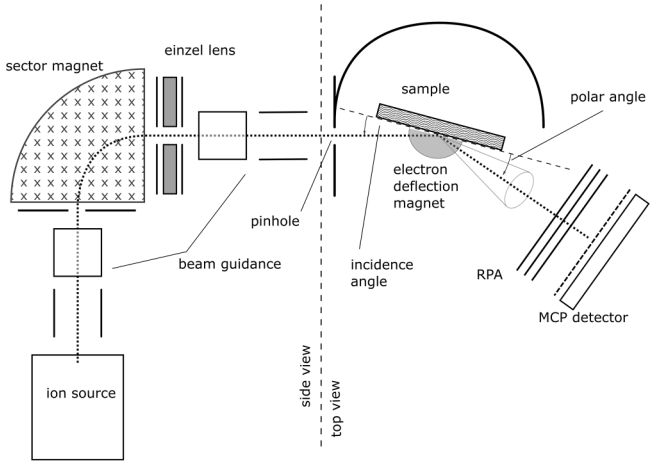

FIG. 1. ILENA measurement setup.

interaction with the CS, a memory loss of the initial charge state of the atom happens,[7,28,37,42] i.e., atoms of different charge state (H^+, H^0, H^-) experience the same scattering and negative ion yield. The interaction can, therefore, be regarded as acting between a neutral atom and the CS. This was also experimentally confirmed in Jans *et al.*[15]

A weak vertical magnetic field is used at the CS to direct released secondary electrons back onto the CS. After charge-exchange interaction with the sample, the particles are scattered toward the MCP detector. A retarding potential analyzer (RPA) prevents positive ions from reaching the detection subsystem; low-energy electrons are rejected likewise by a slight negative potential grid in front of the detector. Therefore, only neutral atoms and negative ions are detected.

The MCP detector itself consists of five consecutive MCPs mounted in front of a quadrilateral resistive anode. A subsequent analog position computing unit determines the location of each detected particle. The entire detector unit, including the RPA, is shielded electrostatically. It can be rotated about the polar axis at the sample holder center from $\theta = 0°$ to 90°. The entire MCP detector may optionally be floated on a high negative potential to reject negatively charged ions.

B. Sample preparation and characterization

The CS sample under test consists of a highly polished Si wafer coated with cadmium telluride (CdTe) of about 35 nm thickness, according to parameters during the fabrication process. Two identical trapezoidal Si wafer facets of about $18 \times 28\,mm^2$ and 1 mm thickness were prepared for coating. Initial surface roughness was about 0.1 nm rms. The CdTe layer was deposited at the Laboratory for Photovoltaics and Solid State Physics, University of Verona, Italy. CdTe was deposited by thermal evaporation in vacuum with a deposition rate of 0.29 nm/s at a pressure of 10^{-5} mbar. CdTe lumps are put in a graphite crucible and brought to a temperature of around 700 °C, the deposition rate, and the thickness is controlled by a quartz thickness monitor. The process duration was 2 min. The substrate temperature reached 90 °C during the coating process. According to Heisler *et al.*,[14] these conditions might result in a slight Te excess of a few percent compared to the nominal stoichiometric ratio (Cd:Te = 1:1), which is not considered relevant for this application. The surface of one CdTe-coated sample was investigated for its roughness using atomic force microscopy (AFM) at the Department of Chemistry and Biochemistry, University of Bern. We measured the surface roughness from AFM scans at three different locations on the sample: one near the center, another one near the lower left rim, and a third near the upper right rim. The AFM operates at ambient conditions with a FlexAFM scan head and a Tap190AI-G cantilever. Each location was scanned twice, with an imaging resolution of 256×256 pixels per $5\,\mu m$ and $1\,\mu m$, respectively.

Figure 2 shows an AFM image of the CdTe surface. It reveals a granular surface structure with about 25 nm grain size. On large scales, the coated surface is homogeneous with only very few small defects. The measured surface roughness was averaged over the total area of three spots, which all showed very similar results for

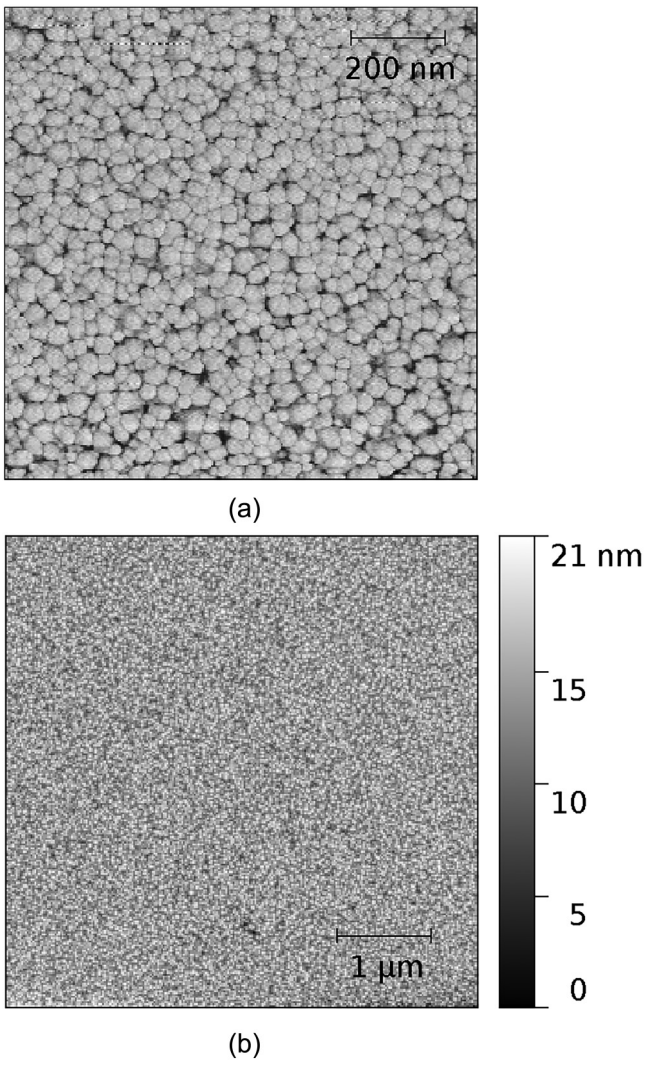

FIG. 2. AFM image of the CdTe surface. (a) Phase image that clearly shows the granular structure. The image area is $1\,\mu m^2$. (b) Grayscale-coded height profile. The image area is $5\,\mu m^2$.

all scanned spots at either imaging resolution. This yields a surface roughness $\mathcal{R}$ of

$$\mathcal{R} = 2.8 \pm 0.05\,nm_{rms}$$

with maximal height differences of about 20 nm peak-to-valley. This is significantly rougher than previous tested samples of different materials, by a factor of 2–3[1,23] to more than a factor of 10.[26,36] Furthermore, we obtained the coating thickness by measuring the height difference at the edge of the coated area, because a margin of about 2 mm remained uncoated. At several places along the coating edge, the surface height was compared

for two points separated about 600 μm across the coating edge. The CdTe coating thickness was measured to be 38.0 $\pm$ 4.0 nm using interferometry.

C. Measurement procedure

After the sample installation, the vacuum chamber was baked out during 48 h at a temperature of $T = 80\,^{\circ}\mathrm{C}$. Before starting a measurement, test gas was inserted into the ion source, which increases the pressure in the vacuum chamber, and held in dynamical equilibrium at a pressure of $(4.0 \pm 0.1) \times 10^{-7}$ mbar. The typical base pressure before gas insertion was $(2.5 \pm 0.5) \times 10^{-8}$ mbar.

An ion beam was produced and ion-optical throughput was optimized using the focusing and deflection plates. For each test gas, a series of five consecutive measurements was performed, alternating between floating and the grounded detector subsystem to keep track of long-term system stability (cf., Fig. 3 in Neuland *et al.*[23]). When high-voltage floating the detector, it only accepts neutrals ($N_h = N_0$), while on ground potential, negative ions and neutrals $N_z = N_- + N_0$ are detected. In each single measurement, at least 10^6 counts were collected to guarantee sufficient statistics.

The negative ionization yield η is then computed[8] from the numbers $\tilde{N}_{(0,-)}$ of neutral atoms and negative ions scattered off the CS,

$$\eta = \frac{\tilde{N}_-}{\tilde{N}_0 + \tilde{N}_-} = 1 - \frac{1}{1 + \alpha \frac{N_-}{N_0}} = 1 - \frac{1}{1 + \alpha \left(\frac{N_z - N_h}{N_h}\right)}, \qquad (2)$$

where the parameter $\alpha = \kappa_0/\kappa_- < 1$ is the ratio of the detection efficiencies of neutrals and negative ions and $N_{(z,h)}$ are the number of counts detected, respectively, with zero and high negative retarding potential. α depends on particle species and energy.[25,32] The values used here lie within the range $0.5 < \alpha < 1$.

In this setup, a possible measured background emerges from recoil sputtered particles off the CS, especially secondary H and O from a persisting thin water layer adsorbed on the surface of the sample in the present pressure range. We use the noble gases He and Ne, with atomic masses comparable to those of H and O, respectively, as a proxy for the sputtering background, and subtract these values from the measured data. Since noble gases do not form stable negative ions, the total measured negative ion yield is considered to be due to sputtering.

For acceleration voltages below 500 V, the efficiency of forming atomic positive hydrogen and oxygen ions in the ion source was too low to achieve reasonably good statistics. Instead, positive molecular ions (H_2^+, O_2^+) were selected and accelerated to twice the nominal energy. This is justified since the vast majority of molecules break up into single atoms during interaction with the CS at the given energies,[15,17,42] so that the measured negative ion yield is essentially the same as for atomic H or O.

We assign an estimated energy uncertainty of $\pm$10% to these data points to take into account that the kinetic energy of the molecule may be unevenly partitioned among the separate atoms in the molecule dissociation upon surface scattering from the CS. The respective time-of-flight spectra can be found in Jans *et al.*[15]

Additionally, the angular distribution of scattered atoms is recorded using the 2D-imaging MCP detector. The full-width at half-maximum (FWHM) in azimuthal (tangentially to the surface) and polar (normal to the surface) direction is measured for all species at various incident energies by reading out the extend of the 50% contour line in the angular distributions.

In a third part, we investigated the effective energy distribution of the scattered ion beam by the retarding potential analysis. For this purpose, the countrate was monitored at constant incident energy E_i while varying the retarding potential in steps of 100 V from 1.3 E_i/q down to 0 V. At high RPA voltage, only the scattered neutral atoms can reach the detector. When lowering the RPA voltage, an increasing amount of negative ions whose energy exceeds the retarding potential will be detected. To close the measurement sequence, data at the highest retarding potential were taken again, and the data were corrected for a slow linear time trend. The energy distribution of scattered negative ions was then computed as the counts difference between adjacent RPA values and is normalized by the constant number of detected neutrals. The energy distribution of scattered neutrals cannot be directly monitored by this method. However, we assume the particle energy distribution does not depend on the charge state, so that the obtained distribution is considered representative for the total set of scattered oxygen ions and atoms.

III. RESULTS AND DISCUSSION

A. Negative ionization yield

The negative ionization yield of H and O atoms upon scattering at a CdTe conversion surface was measured for energies from 195 eV to 1000 eV per atom at an incidence angle of 8°. The results are shown in Fig. 3. Background values measured with He and Ne, respectively, at the same energies are subtracted from the H and O data to account for recoil sputtering of surface atoms. For helium, the measured negative ion yield was 1.7% at 195 eV, increasing to 2.9% at 1000 eV. For neon, the measured negative ion yield was 3.1% at 250 eV and 4.3%–4.6% for energies from 390 eV to 1000 eV. The value at 195 eV could not be measured for Ne due to ion source instability at this low energy. Instead, the same value as for 250 eV was subtracted from oxygen at 195 eV as sputtering background.

We find a negative hydrogen ionization yield of 2%–3% for incident energies between 195 eV and 1000 eV, showing only a slight increase over the energy range within the uncertainties. For oxygen, the negative ionization yield is about 8.6% at 195 eV and increases to about 12.8% at 1000 eV.

The results found here for a CdTe-coated CS are comparable to those found previously for other coatings: Allenbach *et al.*[1] found very similar negative ionization yield for B-doped DLC. Neuland *et al.*[23] likewise report $\eta \simeq 2\%$ for H on metallized DLC, and $\eta = 10\%$–12% for O. Various DLC-coated CS candidates for IBEX were tested by Wahlström *et al.*[36] and slightly higher negative ion yields were found, 11–20% for O, and 2–4% for H. Scheer[30] did a similar investigation using various H-terminated DLC samples that showed comparable results. Negative ion yields for Al_2O_3 were in the same range[26] as in this work for oxygen ($\eta_O = 9\%$ to 13%), but considerably higher for hydrogen ($\eta_H = 3.5\%$ up to 4.6%).

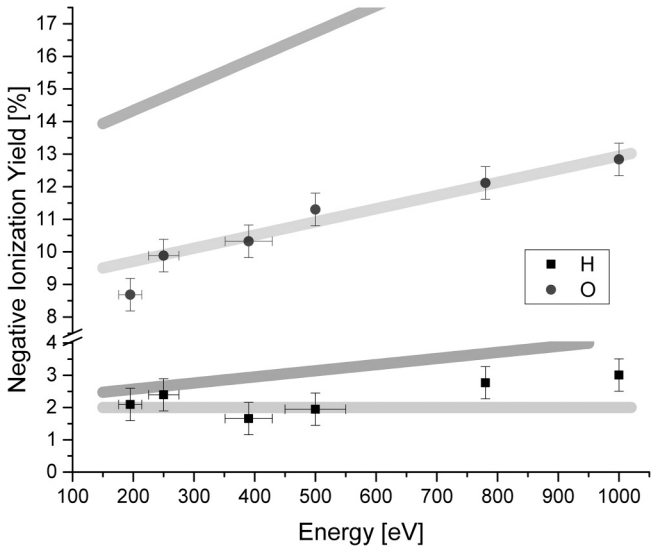

FIG. 3. Negative ionization yield of H and O atoms upon scattering at a CdTe conversion surface under 8° incidence angle for different incident energies per atom. Points with indicated energy uncertainty were done using primary molecular ions with twice the energy. Underlying grayscale bars represent the trends found in previous measurements with DLC samples. Dark gray: results from Scheer *et al.*[30] and Wahlström *et al.*;[36] light gray: results from Neuland *et al.*[23] and Allenbach *et al.*[1]

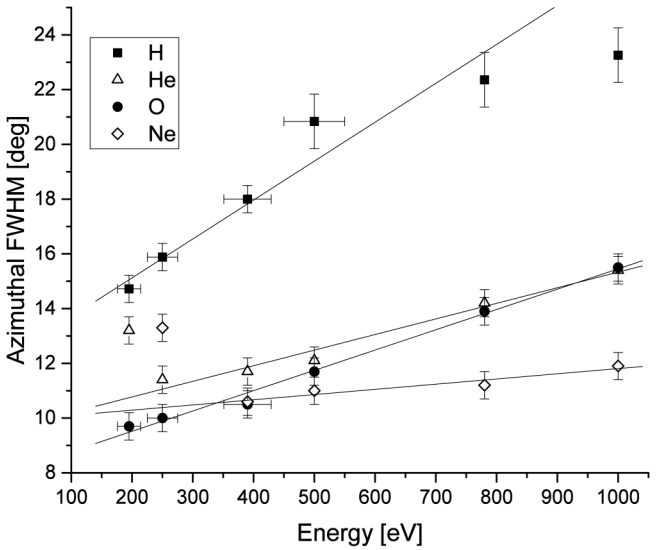

FIG. 4. Azimuthal FWHM of scattered atoms off the CdTe surface at different incident energies at 8° incidence angle. Linear fit lines are shown to guide the eye.

B. Angular scattering distribution

The angular scattering FWHM of H, He, O, and Ne was measured in azimuthal and polar directions for energies from 195 eV to 1000 eV per atom upon scattering on a CdTe-coated CS at an incidence angle of 8°. The results are displayed in Figs. 4 and 5. Hydrogen shows the broadest scattering distribution of more than 14° azimuthal and 16° polar FWHM, while the other species show angular FWHM of 10°–15° in both directions. Values above 20° were on or beyond the detector edge and were obtained using a Gaussian fit in the azimuth direction and a log-normal in the polar direction using a least-squares fit. We estimate a 10% uncertainty in the incident energy per atom for measurements done using molecular primary ions, as explained in Sec. II C.

The angular scattering width increases with particle energy in both angular directions, except for He and Ne at the lowest measured energy. This trend is in accordance with our expectations from previous results with DLC-[1,23,36] and Al_2O_3-coated CS samples.[26,29] While the azimuthal scattering width is usually broader than the polar width by typically about 30%, we see here that for the CdTe-coated CS the azimuthal and polar widths differ by less than 10% for all particle species and energies. The azimuthal widths found here are within the range of angular scattering reported for other coatings. The polar widths are slightly higher compared to the results in Allenbach *et al.*,[1] Neuland *et al.*,[23] Riedo *et al.*,[26] and Wahlström *et al.*[36]

For the application in ENA instruments, a narrow angular scattering cone is strongly favored, as it directly improves the possible instrument throughput of the downstream ion optics. The tested CS sample showed a tolerable but rather high surface roughness in comparison with previous candidates. Moreover, it showed a particular granular structure under the AFM scan rather than a homogeneously smooth surface. While Wahlström *et al.*[36] see no

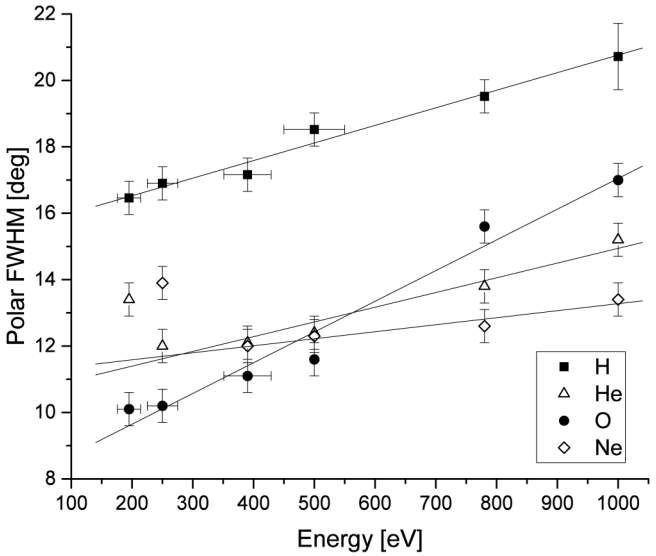

FIG. 5. Polar FWHM of scattered atoms off the CdTe surface at different incident energies at 8° incidence angle. Linear fit lines are shown to guide the eye.

influence of surface roughness on angular scattering, Riedo *et al.*[26] relate broader angular scattering to changes in the surface structure at few Å smooth surfaces, even if the surface roughness increased only insignificantly. This effect will be even larger at rougher surfaces, and angular scattering is expected to be reduced by a smoother coating. This, in turn, depends on the coating process and the underlying Si wafer roughness.

C. Energy distribution

The energy distribution of the scattered particles was investigated using the retarding potential method. A primary O_2^+ ion beam of $E_i = 1000$ eV/q (500 eV per atom) was directed onto the CdTe-coated sample. The fraction of negative ions was then monitored while varying the RPA potential from 1300 V down to 0 V. In Fig. 6, the differential of scattered oxygen ions, normalized to the number of scattered neutral particles, is plotted against the retarding potential.

We observe all negative ions scattered off the CdTe CS at energies below 600 eV. Above ion energies of 500 eV/q, the data are in accordance with zero scattered particles. Small fluctuations are due to statistical variability in the experiment. The RPA measurement shows that all incident molecular ions break up into atoms in the scattering interaction. This agrees with the results found in Wurz *et al.*[42] and Jans *et al.*,[15] where a time-of-flight analysis was used. Otherwise, we should see some fraction of scattered ions still carrying an energy of 500–1000 eV with only some fraction of their energy lost in the scattering process.

The data point around 50 eV is likely dominated by a low-energy component, which originates from ions sputtered off the CS rather than direct scattered O^- ions. This Sigmund–Thompson sputtering background[31] drops off as $\propto E^{-2}$, as indicated in Fig. 6.

The mean energy of scattered O^- ions is about $\langle E \rangle = 273 \pm 30$ eV. This corresponds to a mean energy loss of about $\langle dE/E_i \rangle = 45\%$ for O atoms from primary molecules in the scattering process, which is well in agreement with the energy loss at the IBEX-Lo CS (cf., Fig. 18 in Fuselier *et al.*[9]), where the reported values are $(45 \pm 15)\%$ for O^- ions at about 500 eV.

A similar energy distribution was obtained using primary H_2^+ ions with an energy of 1500 eV, however with a much smaller fraction of scattered negative ions (up to 1%/100 V) and thus much larger relative uncertainties.

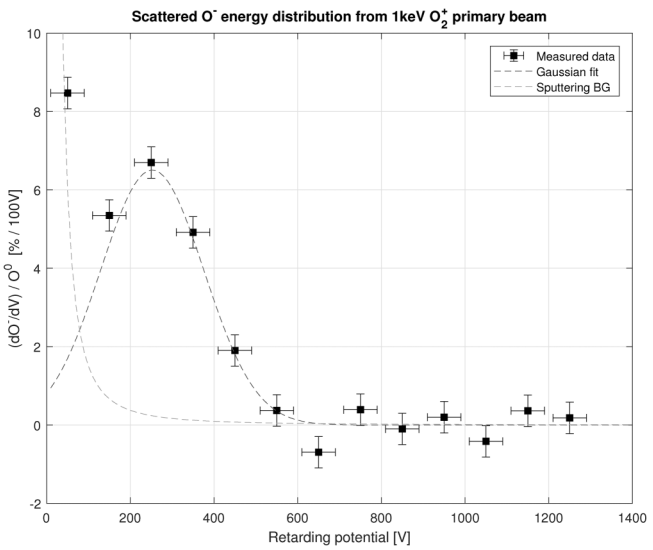

FIG. 6. Energy distribution of scattered O^- ions off the CdTe CS as percentage of total scattered neutral oxygen. The primary O_2^+ ions were accelerated to 1000 eV and were scattered under 8° incidence angle. The low-energetic sputtering background and a Gaussian fit to the scattered O^- energy distribution are indicated.

IV. CONCLUSION

A CdTe-coated Si wafer sample was investigated in the ILENA test facility[35] at University of Bern for its suitability as potential conversion surface in future ENA detection instruments in space research. One key characteristic of a CS is the smoothness on atomic scales. The surface roughness of the CdTe sample under test was investigated by AFM microscopy and was found to be $\mathcal{R} = 2.8$ nm rms, which is near the upper limit for suitable CS as seen from the measurements of angular scatter. Moreover, the granular structure is of concern for the angular and energy scatter. Improvements in the smoothness and homogeneity of the coating are possible in the fabrication process. By chemical (nitro phosphoric or bromine methanol etching) or physical (plasma) etching, it is possible to further reduce the surface roughness. Alternatively, epitaxially grown coating might lead to smoother surfaces.

The scattering properties of the CdTe CS, i.e., the negative ionization yield and the angular scattering width, were measured in the ILENA test facility for various energies at 8° incidence angle. Moreover, the energy distribution of scattered O was recorded. This shows that incident molecular ions are effectively split upon scattering and are scattered as individual atoms. The mean energy loss of about 45% turns out to be higher than previously expected. Our hypothesis that a CS material consisting of heavier atoms compared to C or O could significantly reduce the scattering energy loss could not be confirmed with the present CdTe coating. However, the results are comparable to other CS surfaces in use.

Over all, scattering results for CdTe are comparable to other established CS materials for space applications. Scattered negative ionization yields should exceed at least the 1% threshold for H to get further consideration as a CS.[42] This threshold requirement is readily fulfilled with CdTe. Given that an even smoother coating with CdTe is feasible, it should be possible to reduce angular scattering. In conclusion, we find that CdTe is indeed a possible alternative CS coating material for use in future ENA instruments.

ACKNOWLEDGMENTS

We warmly thank Dr. Vitali Grozovski at DCB, University of Bern, for his great support with AFM microscopy. This work was supported by the Swiss National Science Foundation.

DATA AVAILABILITY

The data that support the findings of this study are available from the corresponding author upon reasonable request.

REFERENCES

[1]M. Allenbach, M. Neuland, A. Riedo, and P. Wurz, Appl. Surf. Sci. **427**, 427 (2017).
[2]S. Barabash, A. Bhardwaj, M. Wieser, R. Sridharan, T. Kurian, S. Varier, E. Vijayakumar, V. Abhirami, K. Raghavendra, S. Mohankumar, M. Dhanya, S. Thampi, K. Asamura, H. Andersson, Y. Futaana, M. Holmström, R. Lundin, J. Svensson, S. Karlsson, and P. Wurz, Curr. Sci. **96**, 526 (2009); available at http://repository.ias.ac.in/64228/
[3]S. Barabash, R. Lundin, H. Andersson, K. Brinkfeldt, A. Grigoriev, H. Gunell, M. Holmström, M. Yamauchi, K. Asamura, P. Bochsler, P. Wurz, R. Cerulli-Irelli, A. Mura, A. Milillo, M. Maggi, S. Orsini, A. Coates, D. Linder, D. Kataria, and J. Thocaven, Space Sci. Rev. **126**, 113 (2006).
[4]S. Barabash, J.-A. Sauvaud, H. Gunell, H. Andersson, A. Grigoriev, K. Brinkfeldt, M. Holmström, R. Lundin, M. Yamauchi, K. Asamura, W. Baumjohann, T. Zhang, A. Coates, D. Linder, D. Kataria, C. Curtis, K. Hsieh, B. Sandel, A. Fedorov, and P. Bochsler, Planet. Space Sci. **55**, 1772 (2007).
[5]S. Barabash, P. Wurz, P. Brandt, M. Wieser, M. Holmström, Y. Futaana, G. Stenberg Wieser, H. Nilsson, A. Eriksson, M. Tulej, A. Vorburger, N. Thomas, C. Paranicas, D. Mitchell, G. Ho, B. Mauk, D. Haggerty, J. Westlake, M. Fränz, and D. Grodent, Proc. Eur. Planet. Sci. Congr. **8**, EPSC2013 (2013); available at https://meetingorganizer.copernicus.org/EPSC2013/EPSC2013-709.pdf
[6]A. Bhardwaj, S. Barabash, Y. Futaana, Y. Kazama, K. Asamura, D. McCann, R. Sridharan, M. Holmström, P. Wurz, and R. Lundin, J. Earth Syst. Sci. **114**, 749 (2005).
[7]D. Faircloth and S. Lawrie, New J. Phys. **20**, 025007 (2018).
[8]M. Föhn, "Application of surface physics for instruments in space science," master thesis (University of Bern, 2017).
[9]S. Fuselier, P. Bochsler, D. Chornay, G. Clark, G. Crew, G. Dunn, T. Friedmann, H. Funsten, A. Ghielmetti, J. Googins, M. Granoff, J. Hamilton, J. Hanley, D. Heirtzler, E. Hertzberg, D. Isaac, B. King, U. Knauss, and S. Zaffke, Space Sci. Rev. **146**, 117 (2009).
[10]Y. Futaana, S. Barabash, X.-D. Wang, M. Wieser, G. S. Wieser, P. Wurz, N. Krupp, and P. Brandt, Planet. Space Sci. **108**, 41 (2015).
[11]M. Gloeckler, I. Sankin, and Z. Zhao, IEEE J. Photovoltaics **3**, 1389 (2013).
[12]M. Green, E. Dunlop, J. Hohl-Ebinger, M. Yoshita, N. Kopidakis, and X. Hao, Prog. Photovoltaics Res. Appl. **28**, 629 (2020).
[13]M. Gruntman, Rev. Sci. Instrum. **68**, 3617 (1997).
[14]C. Heisler, M. Brückner, F. Lind, C. Kraft, U. Reislöhner, C. Ronning, and W. Wesch, J. Appl. Phys. **113**, 224504 (2013).
[15]S. Jans, P. Wurz, R. Schletti, K. Brüning, K. Sekar, W. Heiland, J. Quinn, and R. Leuchtner, Nucl. Instrum. Methods Phys. Res. Sect. B **173**, 503 (2001).
[16]Y. Kazama, S. Barabash, M. Wieser, K. Asamura, and P. Wurz, AIP Conf. Proc. **1144**, 109 (2009).
[17]A. Kleyn, J. Phys. Condens. Matter **4**, 8375 (1992).
[18]W. Lei, J. Antoszewski, and L. Faraone, Appl. Phys. Rev. **2**, 041303 (2015).
[19]J. Los and J. Geerlings, Phys. Rep. **190**, 133 (1990).
[20]D. McComas, F. Allegrini, P. Bochsler, M. Bzowski, M. Collier, H. Fahr, H. Fichtner, P. Frisch, H. Funsten, S. Fuselier, G. Gloeckler, M. Gruntman, V. Izmodenov, P. Knappenberger, M. Lee, S. Livi, D. Mitchell, E. Moebius, T. Moore, S. Pope, D. Reisenfeld, E. Roelof, J. Scherrer, N. Schwadron, R. Tyler, M. Wieser, P. Wurz, and G. Zank, Space Sci. Rev. **146**, 11 (2009).
[21]D. McComas, E. Christian, N. Schwadron, N. Fox, J. Westlake, F. Allegrini, D. Baker, D. Biesecker, M. Bzowski, G. Clark, C. Cohen, I. Cohen, M. Dayeh, R. Decker, G. de Nolfo, M. Desai, R. Ebert, H. Elliott, H. Fahr, and E. Zirnstein, Space Sci. Rev. **214**, 116 (2018).
[22]T. Moore, D. Chornay, M. Collier, F. Herrero, J. Johnson, M. Johnson, J. Keller, J. Laudadio, J. Lobell, K. Ogilvie, P. Rozmarynowski, S. Fuselier, A. Ghielmetti, E. Hertzberg, D. Hamilton, R. Lundgren, P. Wilson, P. Walpole, T. Stephen, B. Peko, B. van Zyl, P. Wurz, J. Quinn, and G. Wilson, Space Sci. Rev. **91**, 155 (2000).
[23]M. Neuland, A. Riedo, J. Scheer, and P. Wurz, Appl. Surf. Sci. **313**, 293 (2014).
[24]S. Orsini, S. Livi, K. Torkar, S. Barabash, A. Milillo, P. Wurz, A. Di Lellis, and E. Kallio; the SERENA team, Planet. Space Sci. **58**, 166 (2008).
[25]B. Peko and T. Stephen, Nucl. Instrum. Methods Phys. Res. Sect. B **171**, 597 (2000).
[26]A. Riedo, M. Ruosch, M. Frenz, J. Scheer, and P. Wurz, Appl. Surf. Sci. **258**, 7292 (2012).
[27]U. Roy, G. Camarda, Y. Cui, R. Gul, A. Hossain, G. Yang, J. Zázvorka, V. Dedic, J. Franc, and R. James, Sci. Rep. **9**, 1620 (2019).
[28]J. Scheer, W. Brüning, T. Fröhlich, P. Wurz, and W. Heiland, Nucl. Instrum. Methods Phys. Res. Sect. B **157**, 208 (1999).
[29]J. Scheer, P. Wahlström, and P. Wurz, Nucl. Instrum. Methods Phys. Res. B **267**, 2571 (2009).
[30]J. Scheer, M. Wieser, P. Wurz, P. Bochsler, E. Hertzberg, S. Fuselier, F. Koeck, R. Nemanich, and M. Schleberger, Adv. Space Res. **38**, 664 (2006).
[31]P. Sigmund, Phys. Rev. **184**, 383 (1969).
[32]T. M. Stephen and B. L. Peko, Rev. Sci. Instrum. **71**, 1355 (2000).
[33]T. Takahashi and S. Watanabe, Nucl. Sci. IEEE Trans. **48**, 950 (2001).
[34]S. Velicu, G. Badano, Y. Selamet, C. Grein, J. Faurie, D. Rafol, and R. Ashokan, J. Electron. Mater. **30**, 711 (2001).
[35]P. Wahlström, J. Scheer, A. Riedo, P. Wurz, and M. Wieser, J. Spacecr. Rockets **50**, 402 (2013).
[36]P. Wahlström, J. Scheer, P. Wurz, E. Hertzberg, and S. Fuselier, J. Appl. Phys. **104**, 034503 (2008).
[37]M. Wieser, P. Wurz, K. Brüning, and W. Heiland, Nucl. Instrum. Methods Phys. Res. Sect. B **192**, 370 (2002).
[38]D. Williams, E. Roelof, and D. Mitchell, Rev. Geophys. **30**, 183, (1992).
[39]H. Winter, Phys. Rep. Rev. Sect. Phys. Lett. **367**, 387 (2002).
[40]P. Wurz, *The Outer Heliosphere: Beyond the Planets* (Copernicus Gesellschaft e.V., Katlenburg-Lindau, 2000), p. 251.
[41]P. Wurz, J. Scheer, and M. Wieser, J. Surf. Sci. Nanotechnol. **4**, 394 (2006).
[42]P. Wurz, R. Schletti, and M. Aellig, Surf. Sci. **373**, 56 (1997).